IJMRRS

International Journal for Multidisciplinary Research, Review and Studies

Volume 1 - Issue 1

2024

A Comprehensive Conformable Mathematical Model of Monkeypox Transmission: Stability, Sensitivity, and the Impact of Vaccination on Human Birth Rate

Syeda Alishwa Zanib[a*], **Rimsha Tariq**[a], **Ibtisaam Ali**[a]

[a] *Department of Mathematics, Riphah International University, Main Satyana Road, Faisalabad 44000, Pakistan.*

[*]**Correspondence**: rimshat536@gmail.com

Abstract

In this study, we develop a deterministic mathematical model to capture the transmission dynamics of the monkeypox virus, incorporating vaccination through a system of differential equations. The model accounts for all key interactions driving the virus's spread across both human and rodent populations. In the human population, the compartments include S_H (susceptible), E_H (exposed), I_H (infected), C_H (confirmed cases), V_H (vaccinated), and R_H (recovered). For rodents, the compartments are S_M (susceptible), E_M (exposed), and I_M (infected). Additionally, we explore the system's fractional-order behavior using fractional-order differential equations for values of $\sigma = 0.2, 0.4, 0.6, 0.8, 1$. This stability analysis demonstrates that the disease-free equilibrium is stable when the basic reproduction number $R_0 < 1$ and unstable when $R_0 > 1$. Sensitivity analysis identifies the critical parameters influencing transmission, with ϕ_H (human contact rate), ρ (fraction of vaccinated immigrants), and ϕ_M (rodent contact rate) as the most influential factors. Furthermore, we examine the local and global stability of equilibrium points and conduct numerical simulations. We also analyze the effect of vaccination on the birth rate *rho*, assessing how vaccination coverage influences population growth and its impact on disease dynamics. The results underscore the importance of enhancing vaccination and isolation strategies to lower the virus's reproduction rate and potentially eliminate the disease.

Keywords: Mathematical model, Differential equations, Monkeypox disease, Stability analysis, Vaccination.

1 Introduction

A disease called monkeypox can affect both people and animals. It belongs to the family of orthopoxviruses, which infect humans and are present in cows. The infectious disease mpox can result in a severe rash, fever, swollen lymph nodes, headaches, back discomfort, muscular aches, and low energy shown in Figure 1. Though most recover totally, some people become seriously ill [1]. The monkeypox virus (MPXV) is the cause of mpox. It is an enclosed double-stranded DNA virus belonging to the family Poxviridae, which also contains the viruses vaccinia, cowpox, variola, and others. It is classified as the Orthopoxvirus genus. Clade I, which includes subclades Ia and Ib, and clade II, which includes subclades IIa and IIb, are the two separate clades of the virus [2].

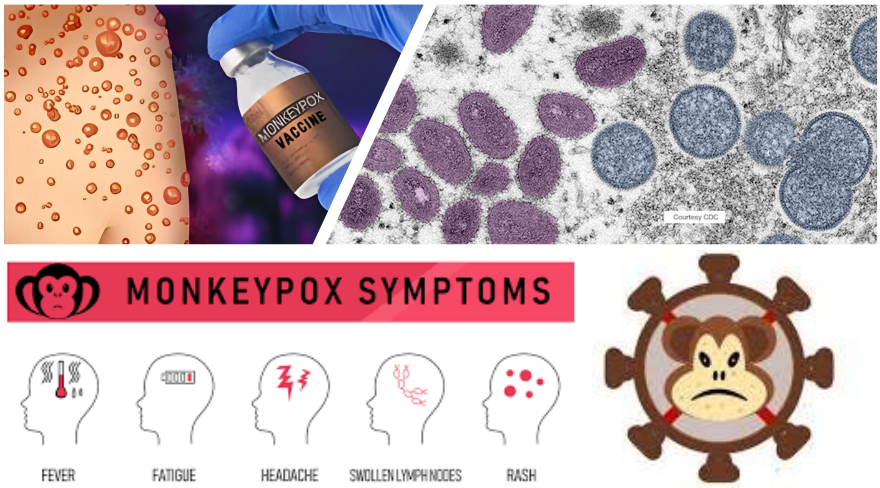

Figure 1: *Monkeypox Disease*

The most serious orthopoxvirus infection since smallpox eradication has been shown to be the monkeypox virus. Since May 2022, there have been over 15,000 confirmed cases of monkeypox from every continent other than Antarctica. Monkeypox was discovered in the 1950s. It was endemic in several regions of western and central Africa prior to this epidemic, and contact with infected animals was usually the cause human illness. The current outbreak is unique in that it is spreading from person to person and has a worldwide reach. Though researchers are still figuring out why this is occurring, several theories include virus mutations, a decline in the smallpox vaccine's use, and changes in behavior [3–5]. Monkeypox can be prevented by a smallpox vaccination, but as smallpox has been eradicated globally, its application is presently limited to clinical studies. Prevention requires limiting human-to-human transmission and minimizing human-animal interaction with infected animals [6]. In order to manage the monkeypox outbreak, it is essential to identify new cases quickly and to monitor and prevent unprotected contact with wild animals, especially those that are sick or dead [7]. In order to forecast future outbreaks of the disease and to extrapolate from current data regarding the state and progression of an outbreak, many researchers now use mathematical models as a suitable and successful strategy. The study of fluid dynamics is essential to understanding fluid flow in the human body, and mathematical biology places a lot of emphasis on blood flow modeling [8–10]. Peter at al (2022) This paper develops a mathematical model of monkeypox using classical and fractional differential equations. It examines stability when $R_0 < 1$ and fits the model to 2019 Nigerian cases. Simulations explore infection dynamics and control policies, highlighting key parameters for eradicating monkeypox [11]. Ashezua & Kaduna (2023)In order to examine how public knowledge, treatment, and immunization impact monkeypox control, this study develops a model. It identifies stable circumstances for both endemic and disease-free states and emphasizes important elements like vaccination rates and transmission rates. Increasing immunization rates and raising awareness can help stop the spread of monkeypox [12]. Okongo at al

(2024) In modeling the transmission of monkeypox in humans and animals, this study denotes disease-free and endemic regions. The reproduction number, R_0, provides the stability. Stemming the monkeypox virus will require managing interactions and prioritizing early diagnosis and treatment [13].
After reviewing the literature, we observe that vaccination is critically important for humans, especially in the presence of clinically ill individuals. Our analysis reveals several gaps in the existing research, particularly concerning the vaccination status of different populations. Notably, we find that immigrants are often vaccinated, while other groups remain unvaccinated, thereby categorizing them as part of the susceptible class. This discrepancy underscores the need for targeted vaccination strategies to protect vulnerable populations and control disease spread effectively. **Section 2:** Transmission model of monkeypox with the vaccine will be examined. We also apply the conformable fractional-order behavior of model. The modified model's reproduction number, local and global stabilities, and monkeypox-free equilibrium point will be examined. **Section 3:** There will be a presentation of the mathematical modeling's results and discussion related to the dynamic interaction. **Section 5:** Conclusion will be discussed in this section.

2 Model formulation

The construct a deterministic mathematical model for the transmission of the monkeypox virus, based on vaccination discussed in this section. The model accounts for interactions between the human and rodent populations. We divide the system into nine compartments: six representing different human groups and three representing the rodent population.
The susceptible human population increases through recruitment via birth or immigration, represented by α_H. It decreases due to the per capita natural death rate β_H and the force of infection ϕ_H and ν_1 is the susceptible person whose take vaccinate. Thus, the rate of susceptible humans changes can be written as:

$$\frac{dS_H}{dt} = \alpha_H\,(1-\rho) + \nu_1\,V_H - (E_H\,\phi_H + \beta_H + \nu_2)\,S_H, \tag{2.1}$$

The number of exposed humans is governed by the force of infection ϕ_H. It decreases at a rate η_H, which represents the transition to becoming infectious, as well as the per capita natural death rate β_H. Therefore, the rate of change in the number of exposed humans is given by:

$$\frac{dE_H}{dt} = \phi_H S_H\,E_H - (\eta_H + \beta_H)\,E_H \tag{2.2}$$

The rate at which the proportion of infected persons rises is $\eta_H E_H$, denoting the change from the exposed to the infectious stage. The decline in this rate can be related to several factors, including the natural death rate β_H, disease-induced death rate ω_1, recovery rate, and the shift to clinically unwell persons at the rate δ. As a result, the pace at which the population of infectious people is changing is:

$$\frac{dI_H}{dt} = \eta_H E_H - (\gamma + \delta + \varpi_1 + \beta_H)\,I_H \tag{2.3}$$

When people in need of medical care exit the infectious compartment at a rate of γ, the number of clinically unwell humans rises. These people transition at a pace of ξ to the recovery stage. Because of the natural mortality rate β_H and the disease-induced death rate ω_2, the number of clinically unwell persons reduces. Thus, the following formula provides the rate of change in the population of clinically unwell humans:

$$\frac{dC_H}{dt} = \gamma\,I_H - (\xi + \varpi_2 + \beta_H)\,C_H \tag{2.4}$$

A fraction ρ of immigrants are vaccinated, whereas the remaining $1-\rho$ are not vaccinated and are therefore classified as susceptible. where θ is the rate at which recovered individuals receive vaccination, and ν_2 represents the rate at which vaccinated individuals can become susceptible.

$$\frac{dV_H}{dt} = \rho\,\alpha_H + \nu_2 S_H + \theta\,R_H - (\nu_1 + \beta_H)\,V_H \tag{2.5}$$

As people transition at the rate δ from the clinically unwell compartment to the recovered compartment, the number of recovered persons increases. Then, as a result of immunity loss at a rate of θ_H and natural mortality at a rate of β_H, this population declines. As a result, the restored human population is changing at the following rate:

$$\frac{dR_H}{dt} = \delta\, I_H - (\theta + \beta_H)\, R_H \tag{2.6}$$

A steady birth rate α_M leads to recruitment of more vulnerable rodents. Through interaction with diseased rodents, represented by ϕ_M, they get the infection. The natural death rate β_M causes the population to decline. Consequently, the vulnerable rodent population's rate of change is:

$$\frac{dS_M}{dt} = \alpha_M - (E_M\, \phi_M + \beta_M)\, S_M \tag{2.7}$$

The force of infection ϕ_M causes an increase in the number of exposed rodents. Together with the natural death rate β_M, it declines at the rate η_M, which denotes the change to the infectious class. Consequently, the number of exposed rodents is changing at the following rate:

$$\frac{dE_M}{dt} = \phi_M S_M\, E_M - (\eta_M + \beta_M)\, E_M \tag{2.8}$$

The number of infectious rodents increases as exposed rodents transition to the infectious state at the rate η_M. It decreases due to the natural death rate β_M. Therefore, the rate of change in the population of infectious rodents is:

$$\frac{dI_M}{dr} = \eta_M E_M - \beta_M I_M \tag{2.9}$$

thus the whole system is as following and schematic diagram show in Figure 2:

$$\begin{cases} \dfrac{dS_H}{dt} = \alpha_H\,(1-\rho) + \nu_1\, V_H - (E_H\, \phi_H + \beta_H + \nu_2)\, S_H, \\ \dfrac{dE_H}{dt} = \phi_H S_H\, E_H - (\eta_H + \beta_H)\, E_H \\ \dfrac{dI_H}{dt} = \eta_H E_H - (\gamma + \delta + \varpi_1 + \beta_H)\, I_H \\ \dfrac{dC_H}{dt} = \gamma\, I_H - (\xi + \varpi_2 + \beta_H)\, C_H \\ \dfrac{dV_H}{dt} = \rho\, \alpha_H + \nu_2 S_H + \theta\, R_H - (\nu_1 + \beta_H)\, V_H \\ \dfrac{dR_H}{dt} = \delta\, I_H - (\theta + \beta_H)\, R_H \\ \dfrac{dS_M}{dt} = \alpha_M - (E_M\, \phi_M + \beta_M)\, S_M \\ \dfrac{dE_M}{dt} = \phi_M S_M\, E_M - (\eta_M + \beta_M)\, E_M \\ \dfrac{dI_M}{dt} = \eta_M E_M - \beta_M I_M \end{cases} \tag{2.10}$$

with initial conditions

$$S_H > 0,\ E_H > 0,\ I_H > 0,\ C_H > 0,\ V_H > 0,\ R_H > 0,\ S_M > 0,\ E_M > 0,\ I_M > 0. \tag{2.11}$$

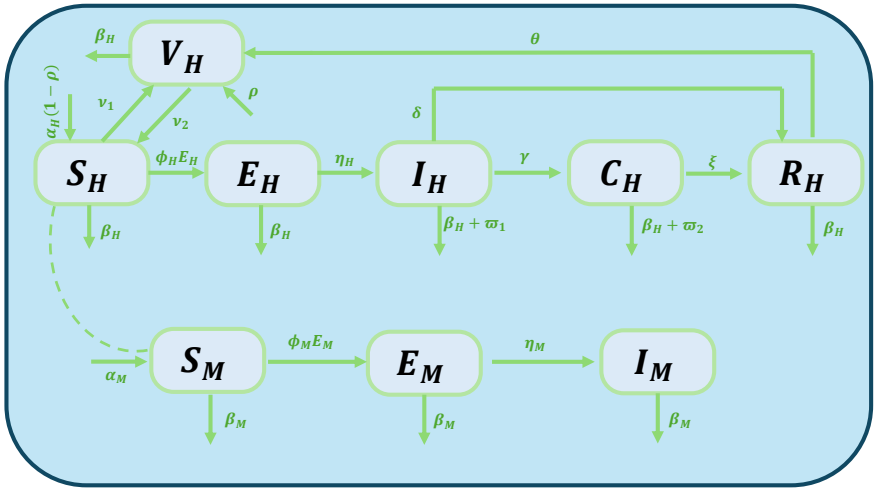

Figure 2: *Monkeypox virus Schematic diagram*

2.1 Positivity of the solution

Suppose that,

$$(S_H(0), E_H(0), V_H(0), I_H(0), C_H(0), R_H(0)) = (S_H^0, E_H^0, V_H^0, I_H^0, C_H^0, R_H^0)$$

be the initial value. and let

$$(S_M(0), E_M(0), I_M(0)) = (S_M^0, E_M^0, I_M^0)$$

represent the state variables' starting values. It follows that

$$(S_H(t), E_H(t), V_H(t), I_H(t), C_H(t), R_H(t), S_M(t), E_M(t), I_M(t))$$

are positive for every time $t > 0$ if $S_M^0, E_M^0, I_M^0, C_M^0, V_H^0, R_H^0$, and S_R^0 are positive. Moreover,

$$\lim_{t\to\infty} \sup N_H(t) \leq \frac{\alpha_H}{\beta_H} \text{ and } \lim_{t\to\infty} \sup N_M(t) \leq \frac{\alpha_M}{\beta_M}.$$

$$\text{Also, if } N_H^0 \leq \frac{\alpha_H}{\beta_H} \leq N_h, \text{ then } N_H \leq \frac{\alpha_H}{\beta_H} \text{ and also, if } N_M^0 \leq \frac{\alpha_M}{\beta_M} \leq N_M, \text{ then } N_H \leq \frac{\alpha_H}{\beta_H}$$

Then, the differential equations have the feasible domain which is given by,

$$\Omega_{N_H} = \left\{ (S_H, E_H, V_H, I_H, C_M, R_H) \subset \mathbb{R}^{+6} : S_H + E_H + V_H + I_H + C_H + R_H \leq \frac{\alpha_H}{\beta_H} \right\} \tag{2.12}$$

$$\Omega_{N_M} = \left\{ (S_M, E_M, I_M) \subset \mathbb{R}^{+3} : S_M + E_M + I_M \leq \frac{\alpha_M}{\beta_M} \right\} \tag{2.13}$$

such that

$$\Omega = \Omega_{N_H} \times \Omega_{N_M} \subset \mathbb{R}^{+6} \times \mathbb{R}^{+3} \tag{2.14}$$

A new definition of fractional derivatives has been proposed by Khalil et al. in [14] and goes as follows:
Definition Supposed that,

$$H : (0, \infty) \to \mathbb{R} \tag{2.15}$$

then the following is the definition of the conformable derivative of H (with order σ):

$$B_\sigma(H)(t) = \lim_{\zeta \to 0} \frac{H(t + \zeta t^{1-\sigma}) - H(t)}{\zeta} \quad \forall t > 0, \quad \sigma \in (0, 1] \tag{2.16}$$

A few properties (listed in [14]) are also satisfied by the given definition. Here is one of such attributes:

Assuming that H is differentiable,

$$B_\sigma(H)(t) = t^{1-\sigma} \frac{dH}{dt} \tag{2.17}$$

Using the previously described Khalil eta al [14] conformable derivative , let's reconstruct the model (2.10) as follows.

$$\begin{cases} B_\sigma(S_H)(t) = \alpha_H\,(1-\rho) + \nu_1\,V_H - (E_H\,\phi_H + \beta_H + \nu_2)\,S_H, \\ B_\sigma(E_H)(t) = \phi_H S_H\,E_H - (\eta_H + \beta_H)\,E_H \\ B_\sigma(I_H)(t) = \eta_H E_H - (\gamma + \delta + \varpi_1 + \beta_H)\,I_H \\ B_\sigma(C_H)(t) = \gamma\,I_H - (\xi + \varpi_2 + \beta_H)\,C_H \\ B_\sigma(V_H)(t) = \rho\,\alpha_H + \nu_2 S_H + \theta\,R_H - (\nu_1 + \beta_H)\,V_H \\ B_\sigma(R_H)(t) = \delta\,I_H - (\theta + \beta_H)\,R_H \\ B_\sigma(S_M)(t) = \alpha_M - (E_M\,\phi_M + \beta_M)\,S_M \\ B_\sigma(E_M)(t) = \phi_M S_M\,E_M - (\eta_M + \beta_M)\,E_M \\ B_\sigma(I_M)(t) = \eta_M E_M - \beta_M I_M \end{cases} \tag{2.18}$$

The operator B_σ in the previously mentioned model, Eqs. (2.22), represents the conformable derivative of the function, with the derivative's order being ($\sigma = (0, 1]$ Now, Eq. (2.17) may be used to convert Eqs. (2.22) as follows:

$$\begin{cases} t^{1-\sigma}\frac{dS_H}{dt} = \alpha_H\,(1-\rho) + \nu_1\,V_H - (E_H\,\phi_H + \beta_H + \nu_2)\,S_H, \\ t^{1-\sigma}\frac{dE_H}{dt} = \phi_H SS\,E_H - (\eta_H + \beta_H)\,E_H \\ t^{1-\sigma}\frac{dI_H}{dt} = \eta_H E_H - (\gamma + \delta + \varpi_1 + \beta_H)\,I_H \\ t^{1-\sigma}\frac{dC_H}{dt} = \gamma\,I_H - (\xi + \varpi_2 + \beta_H)\,C_H \\ t^{1-\sigma}\frac{dV_H}{dt} = \rho\,\alpha_H + \nu_2 S_H + \theta\,R_H - (\nu_1 + \beta_H)\,V_H \\ t^{1-\sigma}\frac{dR_H}{dt} = \delta\,I_H - (\theta + \beta_H)\,R_H \\ t^{1-\sigma}\frac{dS_M}{dt} = \alpha_M - (E_M\,\phi_M + \beta_M)\,S_M \\ t^{1-\sigma}\frac{dE_M}{dt} = \phi_M S_M\,E_M - (\eta_M + \beta_M)\,E_M \\ t^{1-\sigma}\frac{dI_M}{dt} = \eta_M E_M - \beta_M I_M \end{cases} \tag{2.19}$$

Simplifying the previously mentioned gives us the system's final form, which is as follows: with initial

conditions

$$\begin{cases} \frac{dS_H}{dt} = t^{\sigma-1}\left(\alpha_H\left(1-\rho\right)+\nu_1 V_H-\left(E_H\,\phi_H+\beta_H+\nu_2\right)S_H\right), \\ \frac{dE_H}{dt} = t^{\sigma-1}\left(\phi_H S_H\,E_H-\left(\eta_H+\beta_H\right)E_H\right) \\ \frac{dI_H}{dt} = t^{\sigma-1}\left(\eta_H E_H-\left(\gamma+\delta+\varpi_1+\beta_H\right)I_H\right) \\ \frac{dC_H}{dt} = t^{\sigma-1}\left(\gamma\,I_H-\left(\xi+\varpi_2+\beta_H\right)C_H\right) \\ \frac{dV_H}{dt} = t^{\sigma-1}\left(\rho\,\alpha_H+\nu_2 S_H+\theta\,R_H-\left(\nu_1+\beta_H\right)V_H\right) \\ \frac{dR_H}{dt} = t^{\sigma-1}\left(\delta\,I_H-\left(\theta+\beta_H\right)R_H\right) \\ \frac{dS_M}{dt} = t^{\sigma-1}\left(\alpha_M-\left(E_M\,\phi_M+\beta_M\right)S_M\right) \\ \frac{dE_M}{dt} = t^{\sigma-1}\left(\phi_M S_M\,E_M-\left(\eta_M+\beta_M\right)E_M\right) \\ \frac{dI_M}{dt} = t^{\sigma-1}\left(\eta_M E_M-\beta_M I_M\right) \end{cases} \tag{2.20}$$

$$S_H>0,\ E_H>0,\ I_H>0,\ C_H>0,\ V_H>0,\ R_H>0,\ S_M>0,\ E_M>0,\ I_M>0. \tag{2.21}$$

2.2 MonkeyPox-Free Equilibrium (MFE)

The Monkeypox-Free equilibrium (MFE), denoted as $E^0=\left\{S_H^0,E_H^0,I_H^0,C_H^0,V_H^0,R_H^0,S_M^0,E_M^0,I_M^0\right\}$, represents the state where no disease exists within the population. In this equilibrium, all infected compartments are zero.

$$\begin{cases} \alpha_H\left(1-\rho\right)+\nu_1 V_H-\left(E_H\,\phi_H+\beta_H+\nu_2\right)S_H=0, \\ \phi_H S_H\,E_H-\left(\eta_H+\beta_H\right)E_H=0 \\ \eta_H E_H-\left(\gamma+\delta+\varpi_1+\beta_H\right)I_H=0 \\ \gamma\,I_H-\left(\xi+\varpi_2+\beta_H\right)C_H=0 \\ \rho\,\alpha_H+\nu_2 S_H+\theta\,R_H-\left(\nu_1+\beta_H\right)V_H=0 \\ \delta\,I_H-\left(\theta+\beta_H\right)R_H=0 \\ \alpha_M-\left(E_M\,\phi_M+\beta_M\right)S_M=0 \\ \phi_M S_M\,E_M-\left(\eta_M+\beta_M\right)E_M=0 \\ \eta_M E_M-\beta_M I_M=0 \end{cases} \tag{2.22}$$

Therefore, the Monkeypox-Free equilibrium must satisfy this condition, as illustrated in Figure 3

$$\begin{aligned} E^0 &= \left(S_H^0,E_H^0,I_H^0,C_H^0,V_H^0,R_H^0,S_M^0,E_M^0,I_M^0\right) \\ &= \left(\frac{\alpha_M}{\phi_M+\beta_M},,0,0,0,\frac{\alpha_H\left(\left(\phi_H+\beta_H\right)\rho+\nu_2\right)}{{\beta_H}^2+\left(\nu_1+\nu_2+\phi_H\right)\beta_H+\nu_1\phi_H},0,\frac{\alpha_H\left(-\rho\,\beta_H+\beta_H+\nu_1\right)}{{\beta_H}^2+\beta_H\nu_1+\beta_H\nu_2+\beta_H\phi_H+\nu_1\phi_H},0,0\right) \end{aligned} \tag{2.23}$$

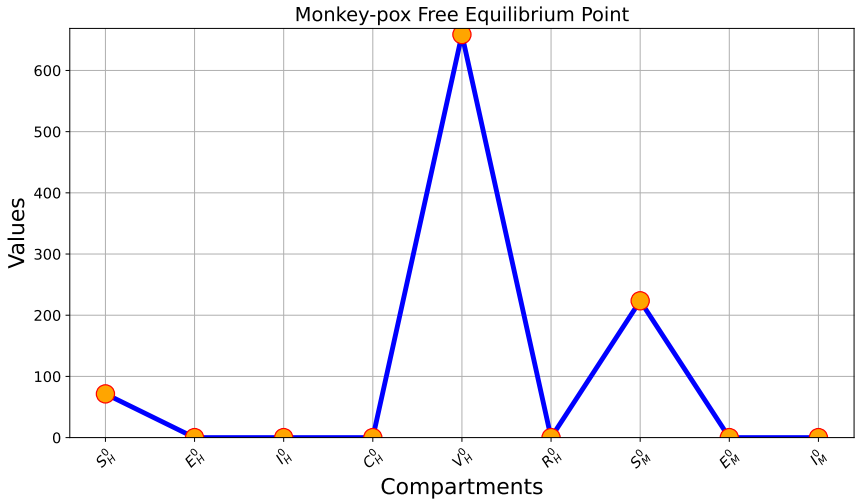

Figure 3: *Graphical representation of MFE*

3 Reproduction number

The next-generation matrix approach will be used to determine the reproduction number. The spectral radius of the next-generation matrix FV^{-1} is the definition of the fundamental reproduction number in accordance with this technique [15]. The fundamental reproduction number is represented by this value.

$$R_0 = \rho(FV^{-1}) \tag{3.1}$$

We thus divide the differential equations into a new infection matrix F and a transfer matrix between compartments, V, using the aforementioned equation (3.1).

$$F = \begin{bmatrix} -\frac{\phi_H \alpha_H (\rho\,\beta_H - \beta_H - \nu_1)}{{\beta_H}^2 + \beta_H \nu_1 + \beta_H \nu_2 + \beta_H \phi_H + \nu_1 \phi_H} & 0 & 0 & 0 & 0 & 0 \\ 0 & 0 & 0 & 0 & 0 & 0 \\ 0 & 0 & 0 & 0 & 0 & 0 \\ 0 & 0 & 0 & 0 & 0 & 0 \\ 0 & 0 & 0 & 0 & \frac{\phi_M \alpha_M}{\phi_M + \beta_M} & 0 \\ 0 & 0 & 0 & 0 & 0 & 0 \end{bmatrix} \tag{3.2}$$

and

$$V = \begin{bmatrix} \eta_H + \beta_H & 0 & 0 & 0 & 0 & 0 \\ -\eta_H & \gamma + \delta + \varpi_1 + \beta_H & 0 & 0 & 0 & 0 \\ 0 & -\gamma & \xi + \varpi_2 + \beta_H & 0 & 0 & 0 \\ 0 & -\delta & 0 & \theta + \beta_H & 0 & 0 \\ 0 & 0 & 0 & 0 & \eta_M + \beta_M & 0 \\ 0 & 0 & 0 & 0 & -\eta_M & \beta_M \end{bmatrix} \tag{3.3}$$

As follows:

$$FV^{-1} = \begin{bmatrix} -\frac{\phi_H \alpha_H (\rho\,\beta_H - \beta_H - \nu_1)}{({\beta_H}^2 + \beta_H \nu_1 + \beta_H \nu_2 + \beta_H \phi_H + \nu_1 \phi_H)(\eta_H + \beta_H)} & 0 & 0 & 0 & 0 & 0 \\ 0 & 0 & 0 & 0 & 0 & 0 \\ 0 & 0 & 0 & 0 & 0 & 0 \\ 0 & 0 & 0 & 0 & 0 & 0 \\ 0 & 0 & 0 & 0 & \frac{\phi_M \alpha_M}{(\phi_M + \beta_M)(\eta_M + \beta_M)} & 0 \\ 0 & 0 & 0 & 0 & 0 & 0 \end{bmatrix} \tag{3.4}$$

The spectral radius can only be ascertained by computing the eigenvalues of FV^{-1}. Using computation and simplification, we get the eigenvalues that are as follows:

$$\begin{bmatrix} 0 \\ 0 \\ 0 \\ 0 \\ \frac{\phi_M \alpha_M}{(\phi_M + \beta_M)(\eta_M + \beta_M)} \\ \frac{\alpha_H (\nu_1 - (\rho-1)\beta_H)\phi_H}{({\beta_H}^2 + (\nu_1 + \nu_2 + \phi_H)\beta_H + \nu_1 \phi_H)(\eta_H + \beta_H)} \end{bmatrix} \tag{3.5}$$

therefore

$$R_0 = \max\left[\frac{\phi_M \alpha_M}{(\phi_M + \beta_M)(\eta_M + \beta_M)},\ \frac{\alpha_H (\nu_1 - (\rho-1)\beta_H)\phi_H}{\left({\beta_H}^2 + (\nu_1 + \nu_2 + \phi_H)\beta_H + \nu_1 \phi_H\right)(\eta_H + \beta_H)}\right] \tag{3.6}$$

Hence,

$$R_0 = \max\left[R_0^M,\ R_0^H\right] \tag{3.7}$$

We examine the following scenarios:

- $\phi_M \alpha_M > (\phi_M + \beta_M)(\eta_M + \beta_M)$ and $\alpha_H (\nu_1 - (\rho-1)\beta_H)\phi_H < \left({\beta_H}^2 + (\nu_1 + \nu_2 + \phi_H)\beta_H + \nu_1 \phi_H\right)(\eta_H + \beta_H)$ then $R_0 > 1$
- $\phi_M \alpha_M < (\phi_M + \beta_M)(\eta_M + \beta_M)$ and $\alpha_H (\nu_1 - (\rho-1)\beta_H)\phi_H > \left({\beta_H}^2 + (\nu_1 + \nu_2 + \phi_H)\beta_H + \nu_1 \phi_H\right)(\eta_H + \beta_H)$ then $R_0 > 1$.
- $\phi_M \alpha_M > (\phi_M + \beta_M)(\eta_M + \beta_M)$ and $\alpha_H (\nu_1 - (\rho-1)\beta_H)\phi_H < \left({\beta_H}^2 + (\nu_1 + \nu_2 + \phi_H)\beta_H + \nu_1 \phi_H\right)(\eta_H + \beta_H)$ then $R_0 > 1$
- $\phi_M \alpha_M < (\phi_M + \beta_M)(\eta_M + \beta_M)$ and $\alpha_H (\nu_1 - (\rho-1)\beta_H)\phi_H < \left({\beta_H}^2 + (\nu_1 + \nu_2 + \phi_H)\beta_H + \nu_1 \phi_H\right)(\eta_H + \beta_H)$ then $R_0 > 1$

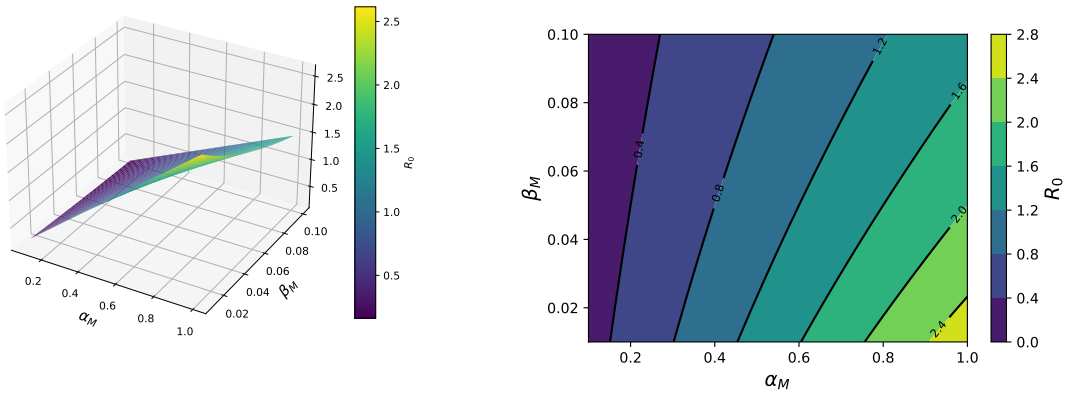

Figure 4: *Behavior of* R_0 *between* α_M *and* β_M

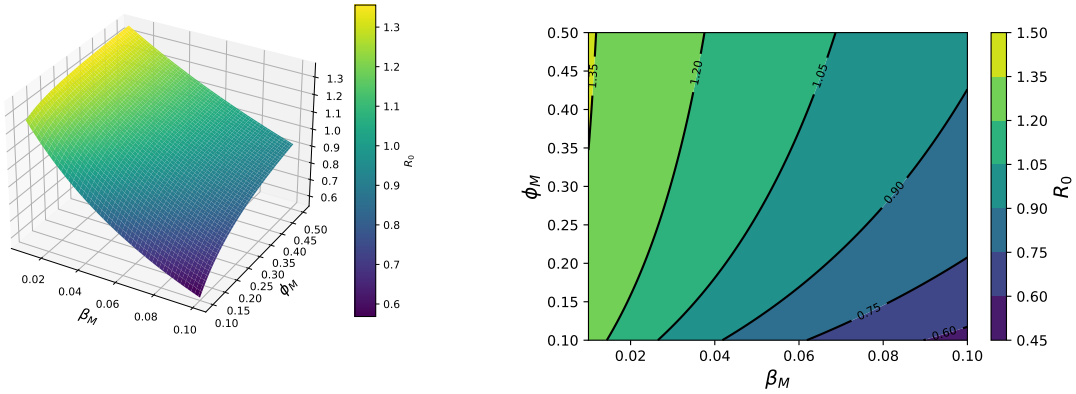

Figure 5: *Behavior of* R_0 *between* ϕ_M *and* β_M

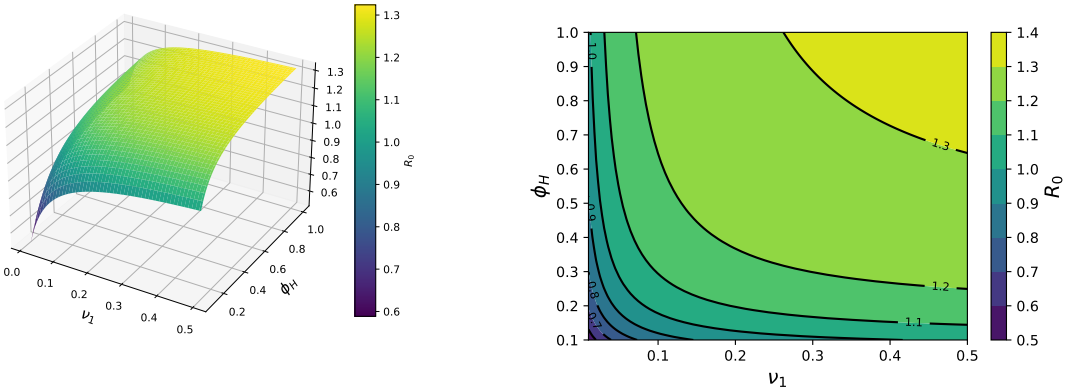

Figure 7: *Behavior of* R_0 *between* ν_1 *and* ϕ_H

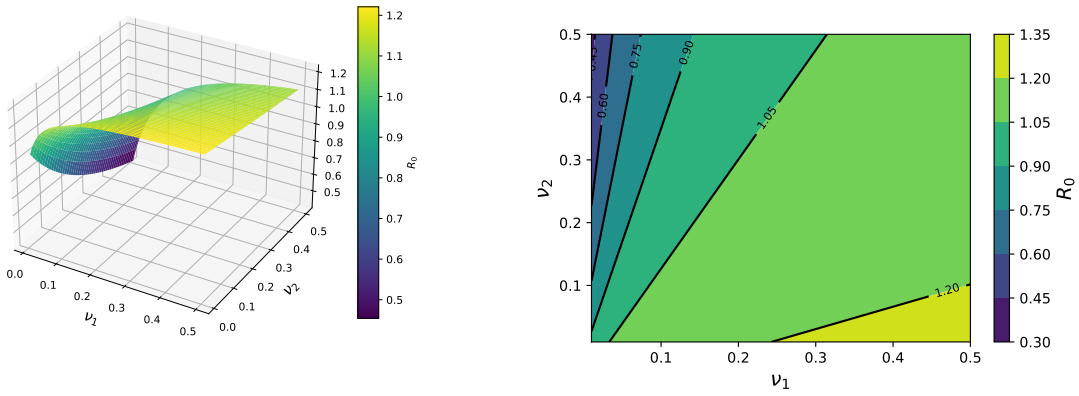

Figure 6: *Behavior of* R_0 *between* ν_1 *and* ν_2

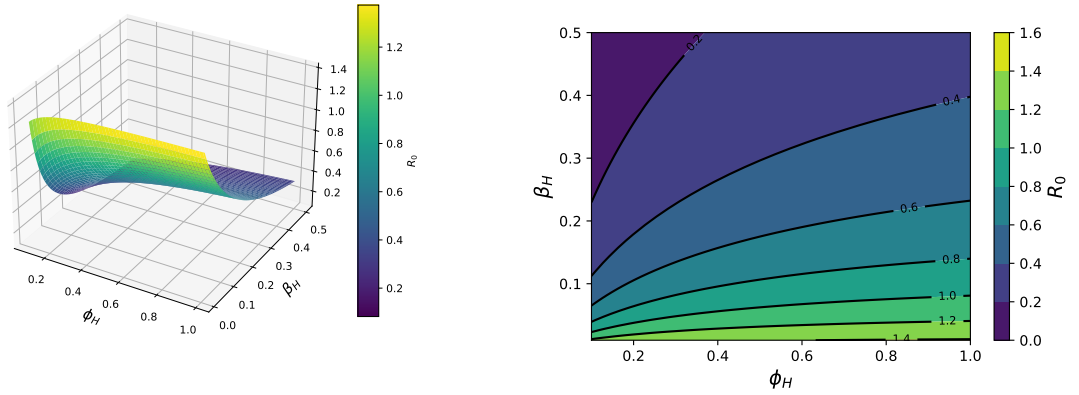

Figure 8: *Behavior of* R_0 *between* ϕ_1 *and* β_H

3.1 Analysis of the basic effective reproduction number (R_0)

To conduct a sensitivity analysis of the basic effective reproduction R_0, we assess how variations in each parameter influence R_0 [16]. This can be achieved by using the normalized forward sensitivity index, which quantifies the relative change in R_0 in response to a relative change in a given parameter. The sensitivity index of $R_0$with respect to a parameter Γ is expressed as:

$$\frac{\partial R_0}{\partial \Gamma} \times \frac{\Gamma}{R_0} \tag{3.8}$$

Next, let's calculate the sensitivity indices for each parameter of rodents.

$$\begin{aligned}
\frac{\partial R_0}{\partial \phi_M} \times \frac{\phi_M}{R_0} &= \frac{\beta_M}{\phi_M + \beta_M} > 0 \\
\frac{\partial R_0}{\partial \alpha_M} \times \frac{\alpha_M}{R_0} &= 1 > 0 \\
\frac{\partial R_0}{\partial \beta_M} \times \frac{\beta_M}{R_0} &= -\frac{\beta_M \left(\eta_M + 2\,\beta_M + \phi_M\right)}{\left(\eta_M + \beta_M\right)\left(\phi_M + \beta_M\right)} < 0 \\
\frac{\partial R_0}{\partial \eta_M} \times \frac{\eta_M}{R_0} &= -\frac{\eta_M}{\eta_M + \beta_M} < 0
\end{aligned} \tag{3.9}$$

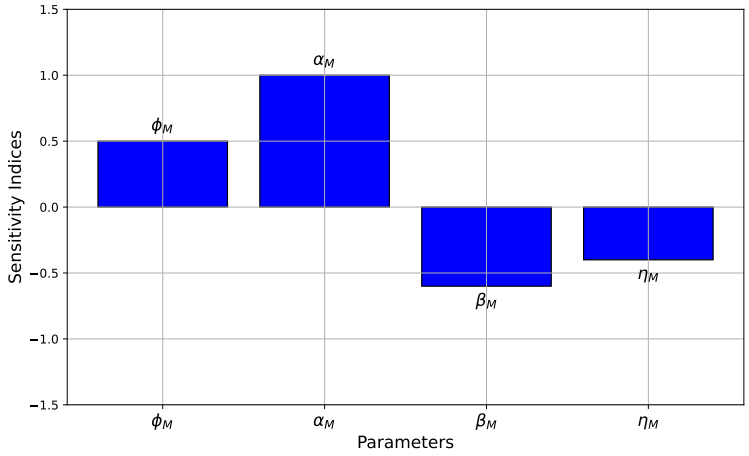

Figure 9: *The Sensitivity Indices of rodents*

Now, let's calculate the sensitivity indices for each parameter of humans.

$$\begin{aligned}
\frac{\partial R_0}{\partial \alpha_H} \times \frac{\alpha_H}{R_0} &= 1 > 0 \\
\frac{\partial R_0}{\partial \beta_H} \times \frac{\beta_H}{R_0} &> 0 \\
\frac{\partial R_0}{\partial \phi_H} \times \frac{\phi_H}{R_0} &= \frac{\beta_H \left(\beta_H + \nu_1 + \nu_2\right)}{{\beta_H}^2 + \left(\nu_1 + \nu_2 + \phi_H\right)\beta_H + \nu_1 \phi_H} > 0 \\
\frac{\partial R_0}{\partial \nu_2} \times \frac{\nu_2}{R_0} &= -\frac{\beta_H \nu_2}{{\beta_H}^2 + \left(\nu_1 + \nu_2 + \phi_H\right)\beta_H + \nu_1 \phi_H} < 0 \\
\frac{\partial R_0}{\partial \nu_1} \times \frac{\nu_1}{R_0} &= -\frac{\nu_1 \beta_H \left(\rho\,\beta_H + \rho\,\phi_H + \nu_2\right)}{\left({\beta_H}^2 + \left(\nu_1 + \nu_2 + \phi_H\right)\beta_H + \nu_1 \phi_H\right)\left(\left(\rho - 1\right)\beta_H - \nu_1\right)} < 0 \\
\frac{\partial R_0}{\partial \rho} \times \frac{\rho}{R_0} &= \frac{\rho\,\beta_H}{\left(\rho - 1\right)\beta_H - \nu_1} > 0
\end{aligned} \tag{3.10}$$

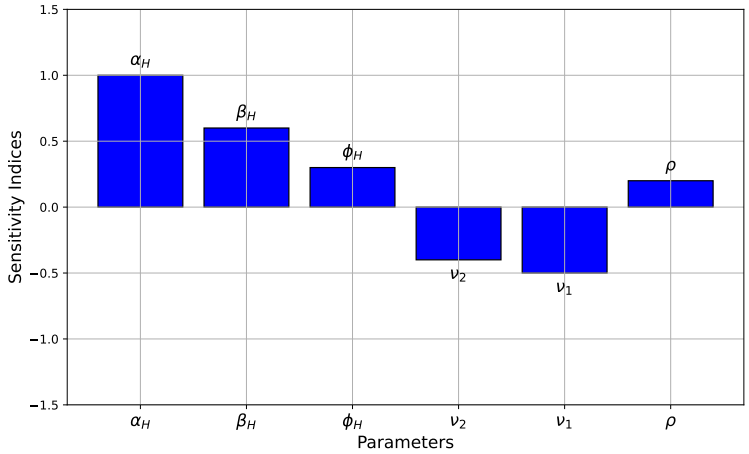

Figure 10: *Sensitivity indices of humans*

3.2 Local Stability of MonkeyPox-Free Equilibrium (MFE)

Theorem 3.1. *The Monkeypox-free equilibrium (MFE) is locally asymptotically stable when* $R_0 < 1$ *and unstable when* $R_0 > 1$.

Proof. To assess the stability of the disease-free equilibrium, we calculate the Jacobian matrix of the system at the MFE and perform a linear stability analysis. This involves computing the eigenvalues, and the signs of these eigenvalues are used to determine stability [17]. We obtain the following by evaluating the Jacobian matrix at the MonkeyPox-Free Equilibrium (MFE), we obtain the following expression:

$$J_E = \begin{bmatrix} -\beta_H - \nu_2 & \nu_1 & j_{1,3} & 0 & 0 & 0 & 0 & 0 & 0 \\ \nu_2 & -\nu_1 - \beta_H & 0 & 0 & 0 & \theta & 0 & 0 & 0 \\ 0 & 0 & J_{3,3} & 0 & 0 & 0 & 0 & 0 & 0 \\ 0 & 0 & \eta_H & -\gamma - \delta - \varpi_1 - \beta_H & 0 & 0 & 0 & 0 & 0 \\ 0 & 0 & 0 & \gamma & -\xi - \varpi_2 - \beta_H & 0 & 0 & 0 & 0 \\ 0 & 0 & 0 & \delta & 0 & -\theta - \beta_H & 0 & 0 & 0 \\ 0 & 0 & 0 & 0 & 0 & 0 & -\beta_M & -\frac{\phi_M \alpha_M}{\phi_M + \beta_M} & 0 \\ 0 & 0 & 0 & 0 & 0 & 0 & 0 & \frac{\phi_M \alpha_M}{\phi_M + \beta_M} - \beta_M - \eta_M & 0 \\ 0 & 0 & 0 & 0 & 0 & 0 & 0 & \eta_M & -\beta_M \end{bmatrix} \tag{3.11}$$

$$j_{1,3} = \frac{\phi_H \alpha_H \left(\rho \beta_H - \beta_H - \nu_1\right)}{{\beta_H}^2 + \beta_H \nu_1 + \beta_H \nu_2 + \beta_H \phi_H + \nu_1 \phi_H}$$

$$j_{3,3} = \frac{\phi_H \alpha_H \left(\rho \beta_H - \beta_H - \nu_1\right)}{{\beta_H}^2 + \beta_H \nu_1 + \beta_H \nu_2 + \beta_H \phi_H + \nu_1 \phi_H} - \beta_H - \eta_H$$

We now calculate the eigenvalues and the characteristic polynomial, expressed as $|J_E - \lambda I|$, where I represents

an 9×9 identity matrix. The resulting eigenvalues, denoted by λ, are obtained as follows:

$$\begin{aligned}
\lambda_1 &= -\beta_H \\
\lambda_2 &= -\beta_H - \nu_1 - \nu_2 \\
\lambda_3 &= \frac{\alpha_M \phi_M - {\beta_M}^2 - \beta_M \eta_M - \beta_M \phi_M - \eta_M \phi_M}{\phi_M + \beta_M} \\
\lambda_4 &= -\xi - \varpi_2 - \beta_H \\
\lambda_5 &= -\theta - \beta_H \\
\lambda_6 &= \frac{-{\beta_H}^3 + (-\nu_1 - \nu_2 - \eta_H - \phi_H)\,{\beta_H}^2 + ((-\nu_1 - \eta_H + (-\rho+1)\,\alpha_H)\,\phi_H - \eta_H\,(\nu_1+\nu_2))\,\beta_H - \nu_1 \phi_H\,(\eta_H - \alpha_H)}{{\beta_H}^2 + (\nu_1 + \nu_2 + \phi_H)\,\beta_H + \nu_1 \phi_H} \\
\lambda_7 &= -\gamma - \delta - \varpi_1 - \beta_H \\
\lambda_8 &= -\beta_M \\
\lambda_9 &= -\beta_M
\end{aligned} \tag{3.12}$$

□

3.3 Global Stability monkey-pox Free Equilibrium Point

Lemma 3.2. *If $R_0 < 1$ (l.a.s.) , then the fixed point $\mathbb{E}_0 = (\mathbb{X}^0, 0)$ system of equations (2.20) is globally asymptotic stable (g.a.s.) if condition **(Z1)** and **(Z2)** conditions are satisfied [18].*

Theorem 3.3. *The model (2.20) is globally asymptotically stable at DEFP E_0 if $R_0 < 1$.*

Proof. Firstly, to satisfy condition **(Z1)**, the model (2.20) are rewrite by setting, $T_H = (S_H, V_H, S_M)$ and, $G_H = (E_H, I_H, C_H, R_H, E_M, I_M)$. Then, disease-free equilibrium point is given by the fixed point, $\mathbb{E}_0 = (\mathbb{X}^0, 0) = \left(\frac{\alpha_M}{\phi_M+\beta_M}, \frac{\alpha_H((\phi_H+\beta_H)\rho+\nu_2)}{{\beta_H}^2+(\nu_1+\nu_2+\phi_H)\beta_H+\nu_1\phi_H}, \frac{\alpha_H(-\rho\,\beta_H+\beta_H+\nu_1)}{{\beta_H}^2+\beta_H\nu_1+\beta_H\nu_2+\beta_H\phi_H+\nu_1\phi_H}\right)$, the system $\frac{dT_H}{dt} = F(T_H, 0)$ becomes,

$$\begin{aligned}
\frac{dS_H^*}{dt} &= \alpha_H(1-\rho) + \nu_1 V_H - (\nu_2 + \phi_H + \beta_H)\,S_H, \\
\frac{dV_H^*}{dt} &= \alpha_H \rho + \nu_2 S_H - (\beta_H + \nu_1)\,V_H, \\
\frac{dS_M^*}{dt} &= \alpha_M - (\phi_M + \beta_M)\,S_M
\end{aligned} \tag{3.13}$$

By solving Eq. (3.13), the equation has a unique equilibrium point,

$$(S_H^*, V_H^*, S_M^*) = \left(\frac{\alpha_M}{\phi_M + \beta_M}, \frac{\alpha_H\,((\phi_H + \beta_H)\,\rho + \nu_2)}{{\beta_H}^2 + (\nu_1 + \nu_2 + \phi_H)\,\beta_H + \nu_1\phi_H}, \frac{\alpha_H\,(-\rho\,\beta_H + \beta_H + \nu_1)}{{\beta_H}^2 + \beta_H\nu_1 + \beta_H\nu_2 + \beta_H\phi_H + \nu_1\phi_H}\right), \tag{3.14}$$

hence $\mathbb{X}^0$ is globally asymptotically stable. So we can say the condition **(Z1)** is fulfilled. Now, to satisfy the second condition **(Z2)**. $H(T_H, G_H) = P_H G_N - \hat{H}(T_H, G_H)$, and $\hat{H}(T_H, G_H) \geq 0$, For that, system of

equations (2.20). We have,

$$G_N = \begin{bmatrix} S_H^* \phi_H - \beta_H - \eta_H & 0 & 0 & 0 & 0 & 0 \\ \eta_H & -\gamma - \delta - \varpi_1 - \beta_H & 0 & 0 & 0 & 0 \\ 0 & \gamma & -\xi - \varpi_2 - \beta_H & 0 & 0 & 0 \\ 0 & \delta & 0 & -\theta - \beta_H & 0 & 0 \\ 0 & 0 & 0 & 0 & S_M^* \phi_M - \beta_M - \eta_M & 0 \\ 0 & 0 & 0 & 0 & \eta_M & -\beta_M \end{bmatrix} \tag{3.15}$$

$$H(T_H, G_H) = \begin{bmatrix} \phi_H S_H E_H - (\eta_H + \beta_H) EE \\ \eta_H E_H - (\gamma + \delta + \varpi_1 + \beta_H) I_H \\ \gamma I_H - (\xi + \varpi_2 + \beta_H) C_H \\ \delta I_H - (\theta + \beta_H) RR \\ S_M \phi_M E_M - (\eta_M + \beta_M) E_M \\ E_M \eta_M - \beta_M I_M \end{bmatrix}, \tag{3.16}$$

$$\hat{H}(T_H, G_H) = P_H G_N - H(T_H, G_H) = \begin{bmatrix} E_H \phi_H (S_H^* - S_H) \\ 0 \\ 0 \\ 0 \\ EM \phi_M (S_E^* - S_E) \\ 0 \end{bmatrix}, \tag{3.17}$$

this shows that, $\hat{H}(T_H, G_H) \geq 0$, where G_N represent an M matrix, it contains a non-negative off-diagonal element. Therefore, the conditions **(Z1)** and **(Z2)** are proved, so by Lemma 3.2 satisfied. Here is the complete proof. □

4 Model result and discussion

With the parameter values listed in Table 2, MATLAB R2018a was used to run and analyze the suggested model. We ran a number of simulations to examine the significance of various factors on the disease's systemic outcomes.We showed the graphical view analysis of the proposed fractional system of monkeypox in Figures 11 and 12. We observe that applying vaccination V_H in the human leads to both an increase in the recovered human R_H rate and a decrease in the number of susceptible individuals S_H. This demonstrates that vaccination plays a crucial role in controlling the spread of the monkeypox virus. By reducing susceptibility and boosting recovery, vaccination can significantly limit disease transmission and improve public health outcomes shown in Figure (11-12).

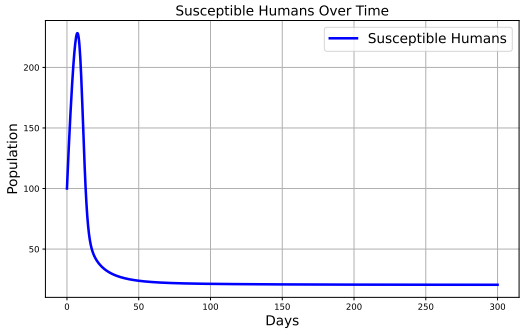

(a) *Susceptible Humans Over Time*

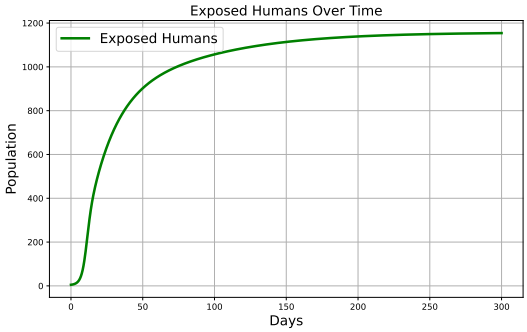

(b) *Exposed Humans Over Time*

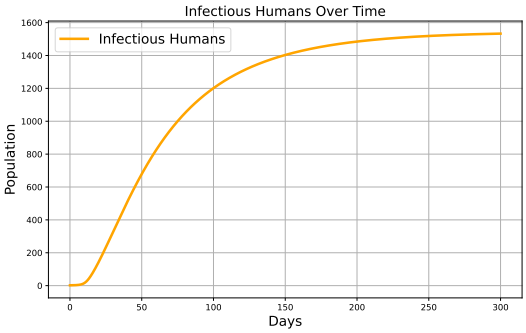

(c) *Infectious Humans Over Time*

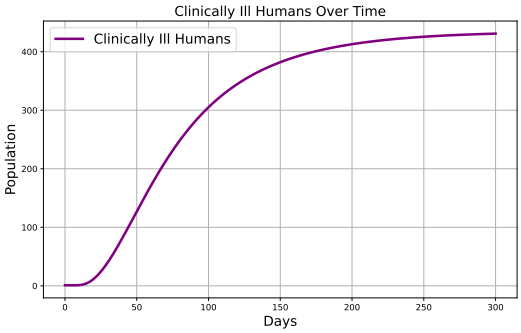

(d) *Clinically Ill Humans Over Time*

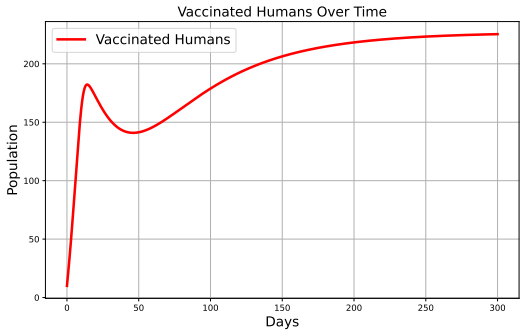

(e) *Vaccinated Humans Over Time*

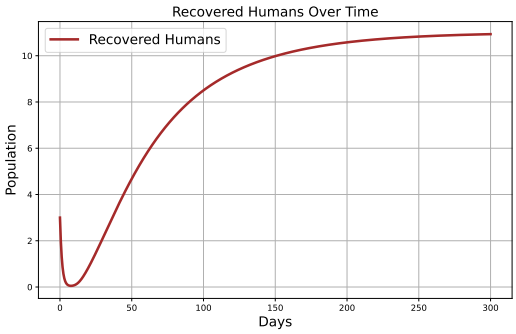

(f) *Recovered Humans Over Time*

Figure 11: *Human Compartments Over Time at classical derivative*

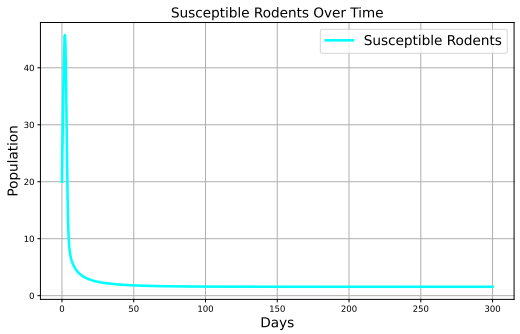

(a) *Susceptible Rodents Over Time*

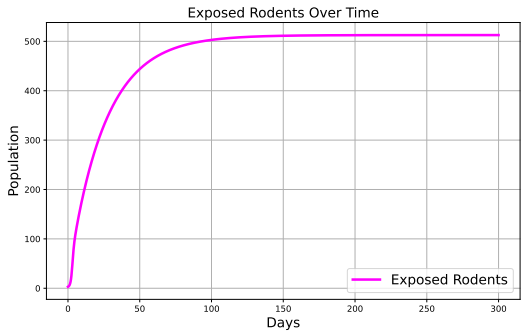

(b) *Exposed Rodents Over Time*

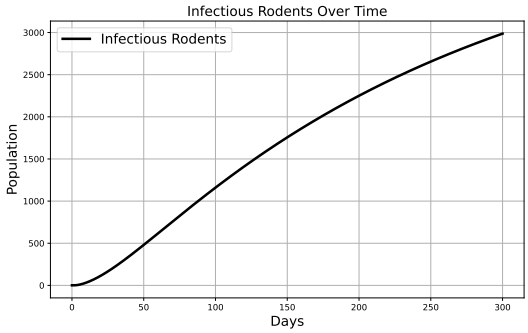

(c) *Infectious Rodents Over Time*

Figure 12: *Rodent Compartments Over Time at classical derivative*

4.1 Fractional-order model (2.20)

The approximate solutions obtained by numerically solving the system of differential equations (2.20) are depicted in the graphs below. The memory effects are shown in these figures for various values of σ. Memory effects cause hidden phenomena to surface when fractional-order derivatives are used; these phenomena are not seen in models with $\sigma = 1$. The benefit of the fractional-order model is that, as the value of σ approaches 1, its solutions (2.20) converge to those of the classical model (2.10).

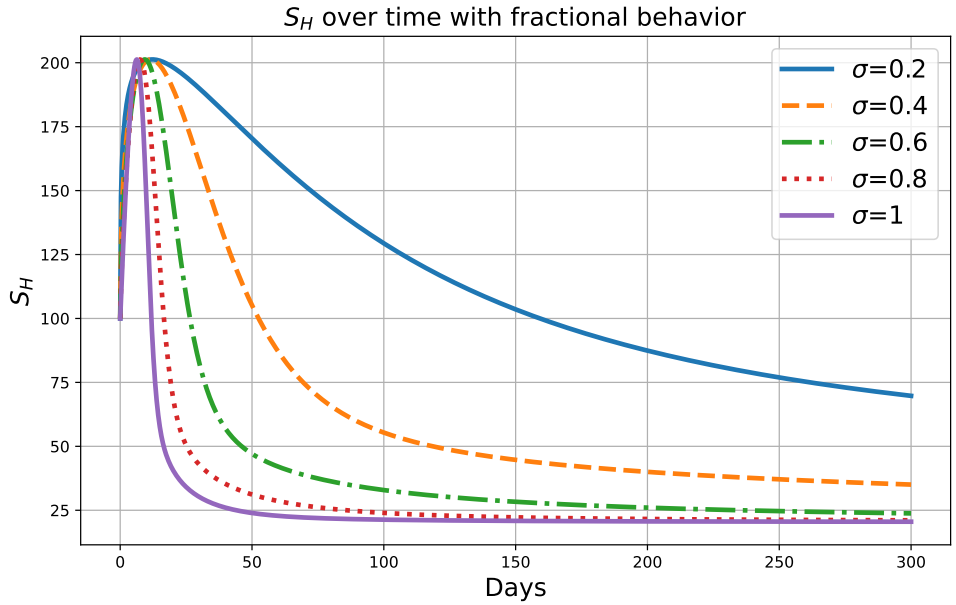

Figure 13: *Fractional dynamics of susceptible individuals in model* (2.20) *for* $\sigma = 0.2, 0.4, 0.6, 0.8, 1$.

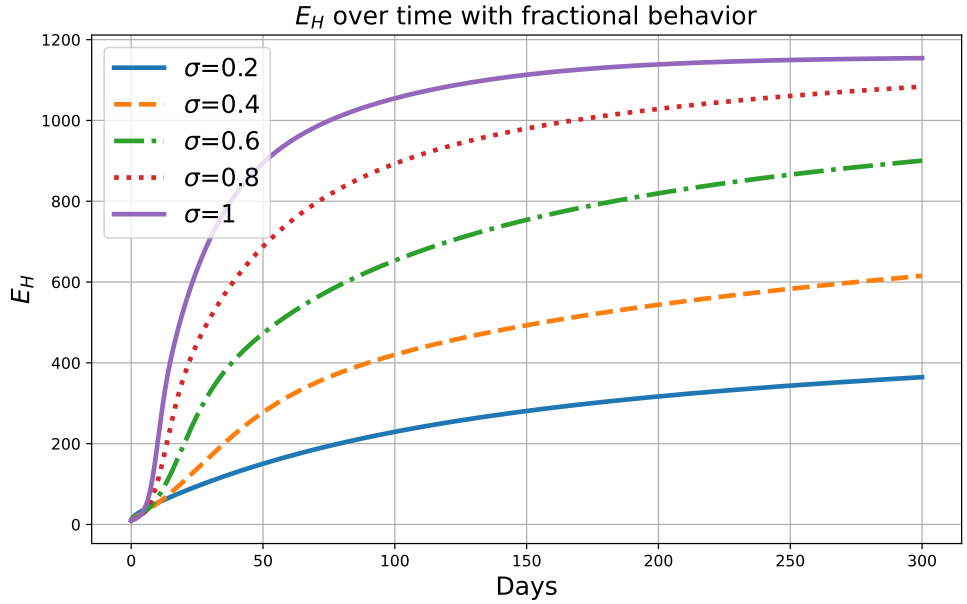

Figure 14: *Fractional dynamics of exposed individuals in model* (2.20) *for* $\sigma = 0.2, 0.4, 0.6, 0.8, 1$

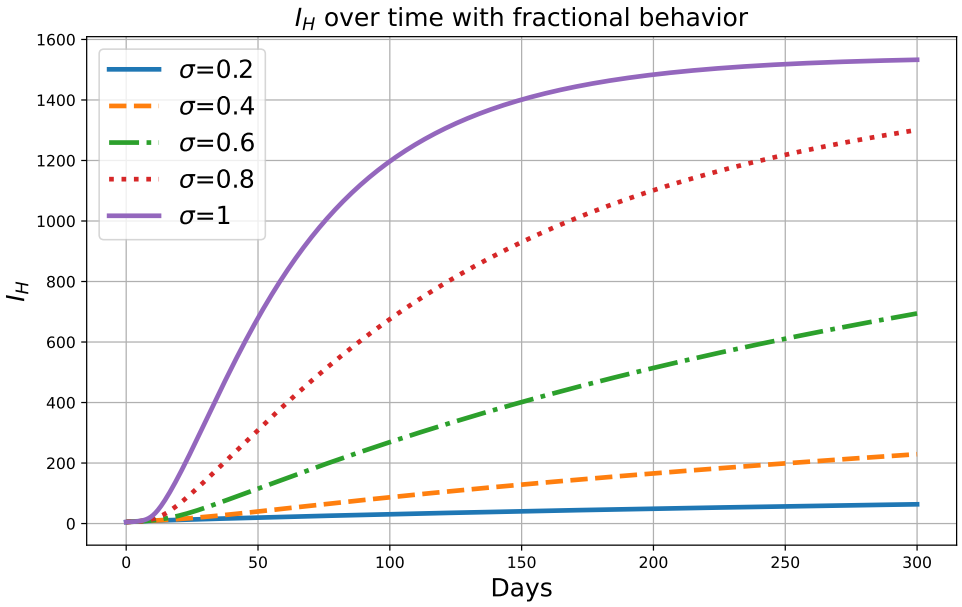

Figure 15: *Fractional dynamics of infectious individuals in model* (2.20) *for* $\sigma = 0.2, 0.4, 0.6, 0.8, 1$

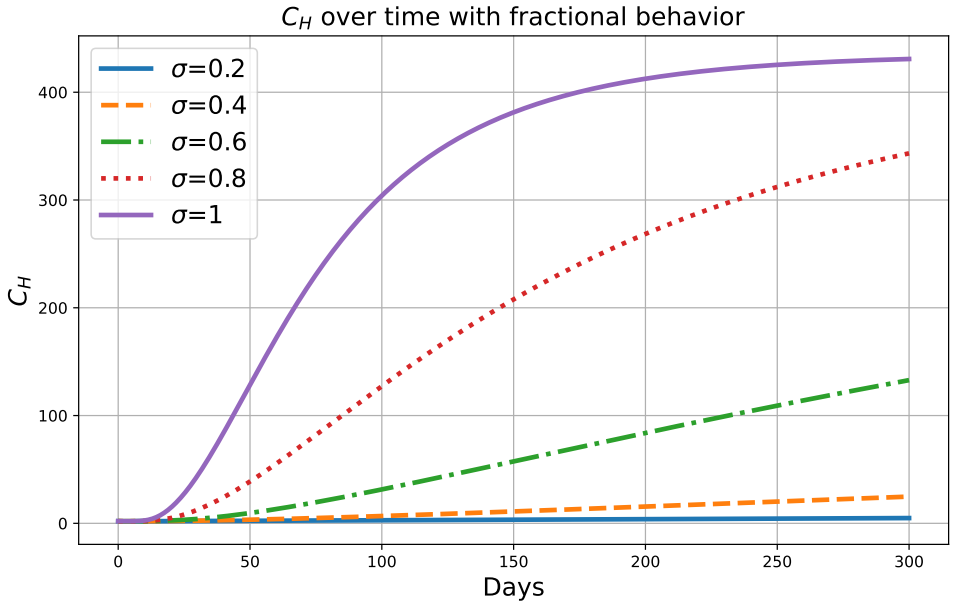

Figure 16: *Fractional dynamics of clinically ill individuals in model* (2.20) *for* $\sigma = 0.2, 0.4, 0.6, 0.8, 1$

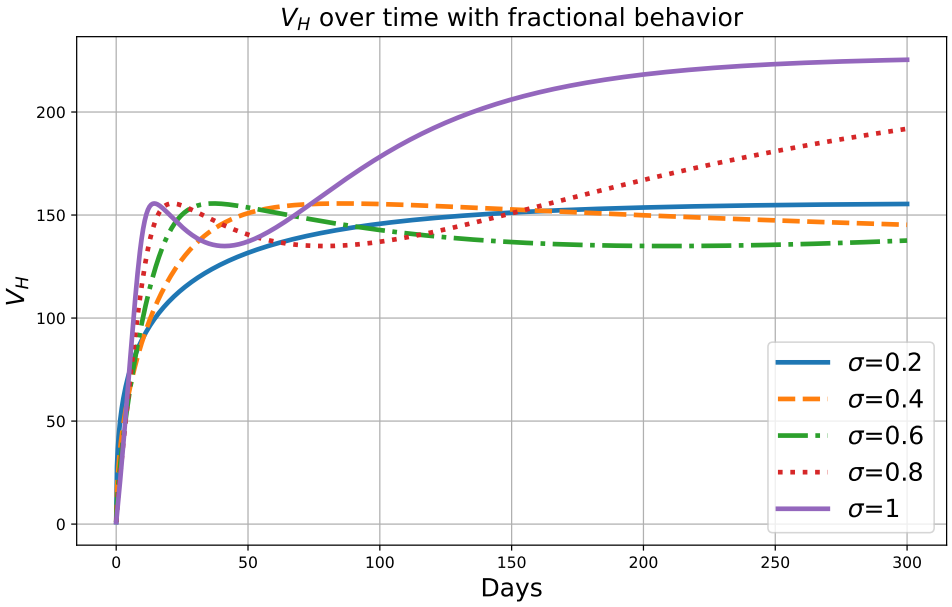

Figure 17: *Fractional dynamics of vaccinated individuals in model* (2.20) *for* $\sigma = 0.2, 0.4, 0.6, 0.8, 1$

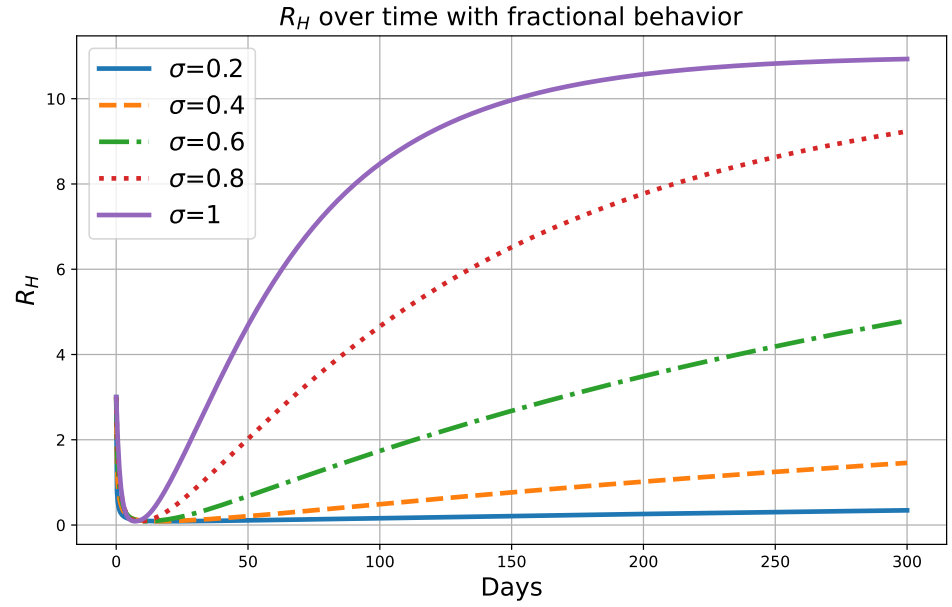

Figure 18: *Fractional dynamics of recovered individuals in model* (2.20) *for* $\sigma = 0.2, 0.4, 0.6, 0.8, 1$

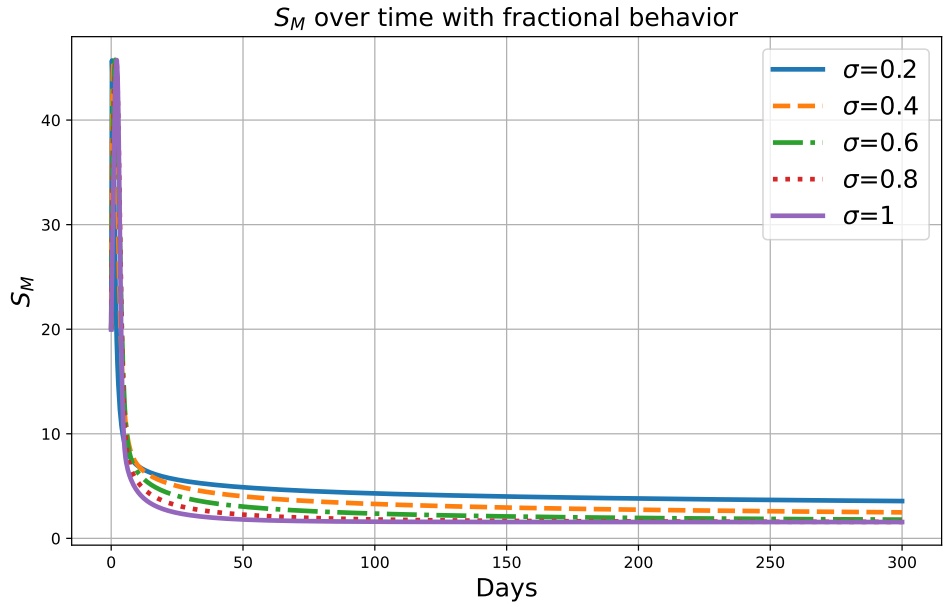

Figure 19: *Fractional dynamics of susceptible rodents in model* (2.20) *for* $\sigma = 0.2, 0.4, 0.6, 0.8, 1$.

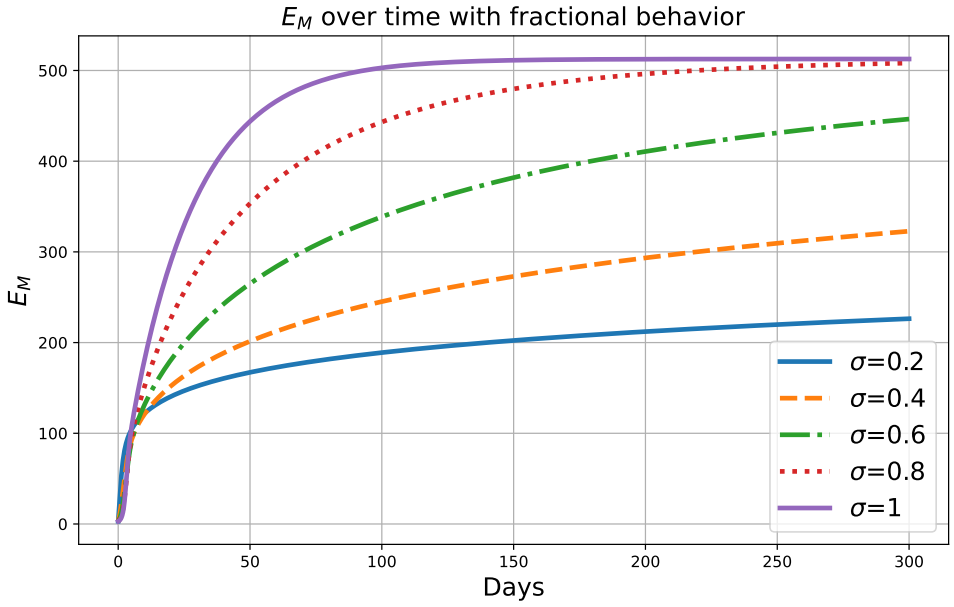

Figure 20: *Fractional dynamics of exposed rodents in model* (2.20) *for* $\sigma = 0.2, 0.4, 0.6, 0.8, 1$.

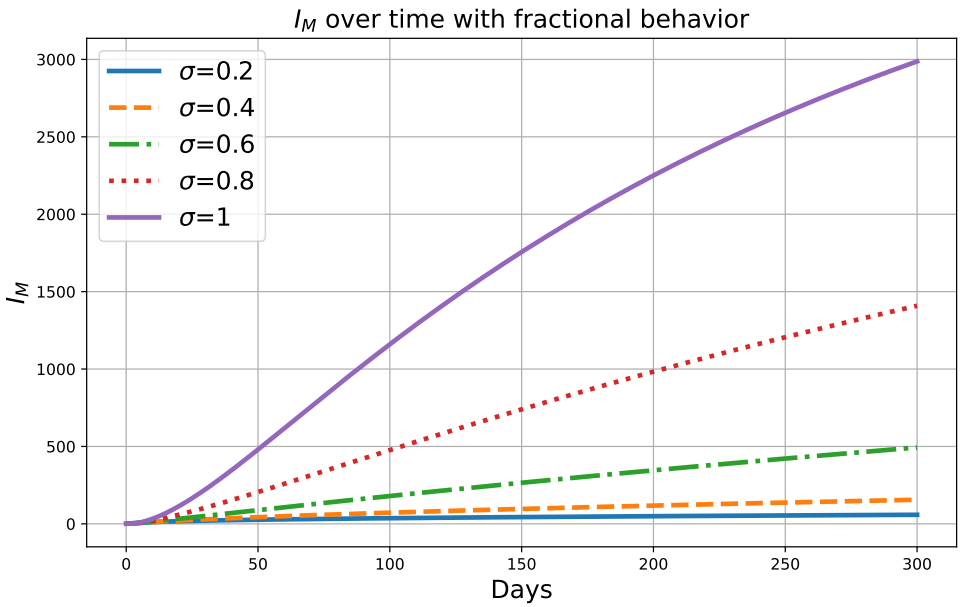

Figure 21: *Fractional dynamics of infected rodents in model* (2.20) *for* $\sigma = 0.2, 0.4, 0.6, 0.8, 1$.

Parameter	**Description**	**Value**
α_H	Human recruitment rate	80
ρ	percentage of vaccinated immigrants	0.02
ν_1	Transition rate to vaccinated	0.2
ν_2	Transition rate from susceptible to vaccinated	0.7
ϕ_H	Transmission rate in humans	0.2
β_H	Natural death rate in humans	0.04
η_H	Progression from exposed to infectious in humans	0.5
γ	Recovery rate for infectious individuals	0.2
δ	Death rate for infectious individuals	0.1
ϖ_1	Mortality due to infection	0.05
ϖ_2	Mortality in clinical cases	0.02
θ	Transition from recovered to vaccinated	0.8
ξ	Natural death rate in clinical individuals	0.06
α_M	Rodent recruitment rate	25
ϕ_M	Transmission rate in rodents	0.3
η_M	Progression from exposed to infectious in rodents	0.45
β_M	Death rate in rodents	0.05

Table 1: *Model parameters and their values*

5 Conclusion

In this work, we introduced a novel deterministic mathematical model to study the transmission dynamics of the monkeypox virus, distinguishing between human and rodent populations. Our analysis demonstrates that the disease-free equilibrium is locally asymptotically stable when the basic reproduction number $R_0 < 1$,

but becomes unstable when $R_0 > 1$, highlighting the importance of controlling this threshold. Through numerical simulations and sensitivity analysis, we explored the impact of key parameters on the spread of monkeypox, identifying critical factors such as human contact rate, rodent interaction, and the fraction of vaccinated immigrants. The findings emphasize that strengthening vaccination and isolation measures can significantly reduce the reproduction rate of the virus, potentially leading to its eradication. The model's stability analysis, in conjunction with its numerical simulations, offers valuable insights into the control strategies required to manage monkeypox outbreaks effectively. This research contributes to our understanding of the virus's transmission mechanisms and provides practical recommendations for public health interventions aimed at preventing and controlling future outbreaks.

Data availability
Not applicable.
Funding
No funding.

References

[1] S. Essbauer, M. Pfeffer and H. Meyer, Zoonotic poxviruses, Vet. Microbiol. 140(3–4) (2010) 229–236.

[2] O'Neill, M., LePage, T., Bester, V., Yoon, H., Browne, F., & Nemec, E. C. (2023). Mpox (formally known as monkeypox). Physician Assistant Clinics, 8(3), 483.

[3] L.A. Learned, M.G. Reynolds, D.W. Wassa, Y. Li, V.A. Olson, K. Karem, L.L. Stempora, Z.H. Braden, R. Kline, A. Likos et al., Extended inte rhuman transmission of monkeypox in a hospital community in the republic of the congo, 2003. Am. J. Trop. Med. Hyg. 73(2), 428–434 (2005)

[4] G.D. Huhn, A.M. Bauer, K. Yorita, M.B. Graham, J. Sejvar, A. Likos, I.K. Damon, M.G. Reynolds, M.J. Kuehnert, Clinical characteristics of human monkeypox, and risk factors for severe disease. Clin. Infect. Dis. 41(12), 1742–1751 (2005)

[5] Z. Ježek, B. Grab, M. Szczeniowski, K. Paluku, M. Mutombo, Clinico-epidemiological features of monkeypox patients with an animal or human source of infection. Bull. World Health Organ. 66(4), 459 (1988).

[6] World Health Organization. (2022). Vaccines and immunization for monkeypox: interim guidance, 24 August 2022 (No. WHO/MPX/Immunization/2022.2). World Health Organization.

[7] Michael, U. E., Omenyi, L. O., Kafayat, E., Nwaeze, E., Akachukwu, O. A., Ozoigbo, G., & Ekhator, M. (2023). Monkeypox mathematical model with surveillance as control. Commun. Math. Biol. Neurosci., 2023, Article-ID

[8] M. Bhatti, S.I. Abdelsalam, Scientific breakdown of a ferromagnetic nanofluid in hemodynamics: enhanced therapeutic approach. Math. Model. Nat. Phenom. 17, 44 (2022)

[9] S.I. Abdelsalam, A. Zaher, On behavioral response of ciliated cervical canal on the development of electroosmotic forces in spermatic fluid. Math. Model. Nat. Phenom. 17, 27 (2022)

[10] V. Sridhar, K. Ramesh, M. Gnaneswara Reddy, M.N. Azese, S.I. Abdelsalam, On the entropy optimization of hemodynamic peristaltic pumping of a nanofluid with geometry effects. Waves Random Complex Media (2022).

[11] Peter, O. J., Oguntolu, F. A., Ojo, M. M., Olayinka Oyeniyi, A., Jan, R., & Khan, I. (2022). Fractional order mathematical model of monkeypox transmission dynamics. Physica Scripta, 97(8), 084005.

[12] Ashezua, T. T., Gweryina, R. I., & Kaduna, F. S. (2023). Population dynamics of a mathematical model for monkeypox. International Journal of Mathematical Analysis and Modelling, 6(1).

[13] Okongo, W., Okelo, J. A., Gathungu, D. K., Moore, S. E., & Nnaemeka, S. A. (2024). Transmission Dynamics of Monkeypox Virus With Age-Structured Human Population: A Mathematical Modeling Approach. Journal of Applied Mathematics, 2024(1), 9173910

[14] Khalil, R., Al Horani, M., Yousef, A., & Sababheh, M. (2014). A new definition of fractional derivative. *Journal of computational and applied mathematics, 264,* 65-70.

[15] Ramzan, S., Rashid, S., Shah, M. A., & Elagan, S. K. (2024). Exploring the dynamical bifurcation and stability analysis of Nipah virus; novel perspectives utilizing fractional calculus. *Modeling Earth Systems and Environment, 10*(4), 5427-5448.

[16] Ma, C., Li, X., Zhao, Z., Liu, F., Zhang, K., Wu, A., & Nie, X. (2022). Understanding dynamics of pandemic models to support predictions of COVID-19 transmission: parameter sensitivity analysis of SIR-type models. *IEEE Journal of Biomedical and Health Informatics, 26*(6), 2458-2468.

[17] Ansori, F. (2024). Mathematical Modeling and Sensitivity Analysis of COVID-19 and Tuberculosis Coinfection with Vaccination. *Mathematical Modelling of Engineering Problems, 11*(1).

[18] Castillo-Chavez C., Blower S., Driessche P., et al. *Mathematical approaches for emerging and reemerging infectious diseases: models, methods, and theory.* (Vol.126). Springer Science & Business Media, 2002.